Photoelectron Spectroscopy of Chloro-Substituted Phenylnitrene Anions

Neloni R. Wijeratne,[†] Maria Da Fonte,[†] Alan Ronemus,[†] Phillip J. Wyss,[†] Daryoush Tahmassebi,[‡] and Paul G. Wenthold*[,†]

Department of Chemistry, Purdue University, West Lafayette, Indiana 47906, and Department of Chemistry, Indiana University−Purdue University Fort Wayne, Fort Wayne, Indiana 46805

Received: April 29, 2009; Revised Manuscript Received: July 8, 2009

The 355 nm time-of-flight negative ion photoelectron spectra of (*o*-, *m*-, and *p*-chlorophenyl)nitrene radical anions are reported. Electron affinities are obtained from the photoelectron spectra, and are 1.79 ± 0.05, 1.82 ± 0.05, and 1.72 ± 0.05 eV for the (*o*-, *m*-, and *p*-chlorophenyl)nitrenes, respectively. Singlet−triplet splittings are determined to be 14 ± 2, 15 ± 1, and 14 ± 2 kcal/mol, respectively. The shapes of the photoelectron bands indicate resonance interactions in the singlet states for the ortho- and para-substituted isomers, which is attributed to quinoidal structures of the open-shell singlet states. Reanalysis of the photoelectron spectrum of phenylnitrene anion leads to a revised experimental singlet−triplet splitting of 14.8 kcal/mol in the unsubstituted phenylnitrene.

Introduction

Nitrenes are unusual reactive intermediates, consisting of monovalent nitrogen, and are isoelectronic with carbenes.[1−5] Although both carbenes and nitrenes can be generated by either thermal or photochemical decomposition of nitrogen containing precursors,[1−4] they have different thermochemical properties and chemical reactivities. For example, whereas aromatic carbenes react with alcohols, alkenes, aromatics, and normally unreactive C−H bonds to form adducts quite efficiently,[1,4] such as the reaction of phenylcarbene, **PC**, with alkenes to give cyclopropanes (eq 1a),[6−8] photolysis of phenyl azide (**PA**) in the presence of alkenes, alcohols, and aromatics results in the formation of polymeric tar (eq 1b).[4,5,9]

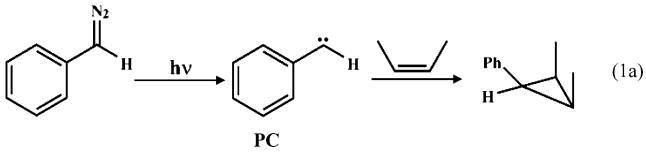

(1a)

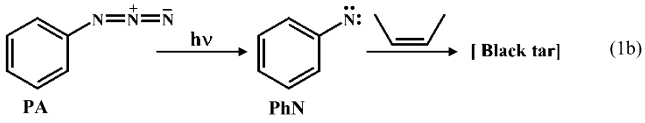

(1b)

Although simple alkyl and aryl carbenes[10−14] and alkyl and aryl nitrenes[1,14−25] have triplet ground states with similar orbital occupancies, there are important differences in the electronic structures of the singlet states.[2,4,26] The lowest energy singlet of phenylcarbene, for example, is a closed-shell state where both electrons occupy the in-plane (σ) orbital, calculated to lie 4 kcal/mol[27−30] higher in energy than the triplet. The singlet state of phenylnitrene (**PhN**), however, is an open-shell ($\sigma\pi$) singlet,[21−23,31] ca. 15 kcal/mol higher in energy than the triplet but 20 kcal/mol below the closed-shell singlet state.[17,23]

[†] Purdue University.
[‡] Indiana University−Purdue University Fort Wayne.

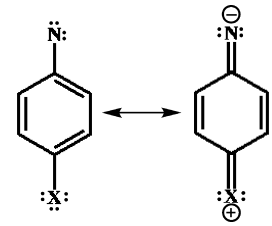

Figure 1. Resonance stabilization of the closed-shell singlet states in para-substituted phenylnitrenes.

Platz and co-workers[1,4] have proposed that the difference in reactivity between phenylcarbene and phenylnitrene arises because of the singlet electronic structure differences. The singlet state of phenylcarbene initially formed upon photolysis or pyrolysis rapidly undergoes intersystem crossing (ISC) to the triplet state, which undergoes clean bimolecular chemistry.[4,22] In contrast, ISC between the open-shell singlet state of phenylnitrene and the triplet is disfavored,[32] such that intermolecular rearrangement of the singlet nitrene occurs faster than ISC.

A potential strategy for taming the reactivity of phenylnitrene is to introduce substituents that can preferentially stabilize the closed-shell singlet state to where it is lower in energy than the open-shell singlet, thereby creating favorable ISC. Substituents that are good π-donors could be used to this effect because π-donors in the para-position are able to stabilize the closed-shell singlet via quinoidal resonance forms,[33] as shown in Figure 1. In contrast, the open-shell states would not be expected to benefit from this type of stabilization. Indeed, Gritsan et al.[34] and Albini and co-workers[33] have shown experimentally that *p*-methoxy- and *p*-amino-substituted phenylnitrenes readily undergo ISC and/or hydrogen abstraction, suggesting that their singlet states are qualititatively different from the meta-substituted isomers, or those with other substituents. With (*p*-chlorophenyl)nitrene,[2,34] the results were more similar to those for the unsubstituted system, suggesting the chlorine is not a strong enough π-donor to sufficiently stabilize the closed-shell singlet.

The substituent effects on the electronic structures of aromatic nitrenes have been investigated computationally by Cramer and

10.1021/jp9039594 CCC: $40.75
Published on Web 08/05/2009

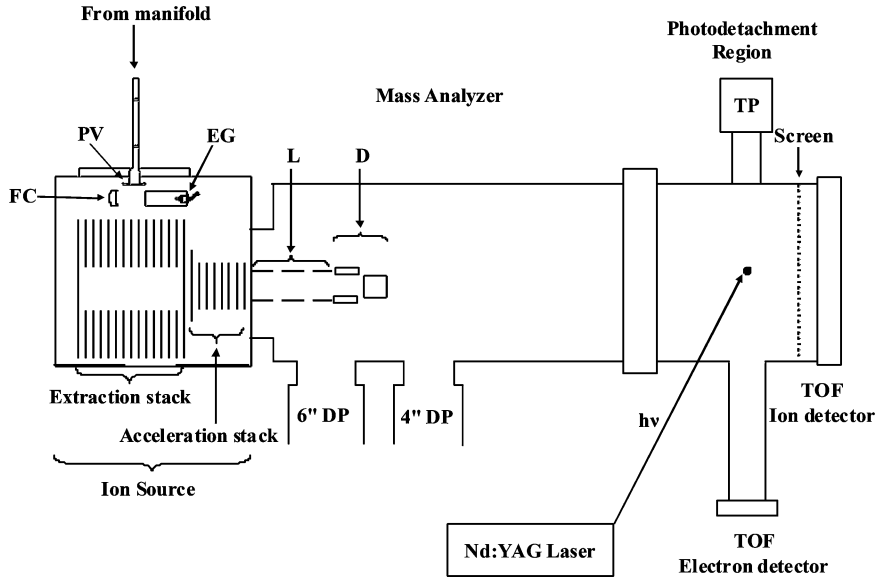

Figure 2. Schematic diagram of the Purdue time-of-flight negative ion photoelectron spectrometer. FC = Faraday cup, EG = electron gun, PV = pulsed valve, DP = diffusion pump, L = Einzel lenses, D = horizontal and vertical deflectors, TP = turbo pump.

co-workers,[22] who compared the relative energies of the triplet, open-shell singlet, and closed-shell states. In contrast with the assessment based on reactivity studies, they found that all of the aromatic nitrenes they examined, including *p*-methoxy and *p*-dimethylamino, had open-shell states as the lowest energy singlets, with singlet−triplet splittings similar to that in phenylnitrene itself. Whereas the closed-shell singlet states in nitrenes with π-donor groups were stabilized, they were still calculated to be >12 kcal/mol higher in energy than the open-shell singlet states, even for the strongest π-donors. The computational results do not necessarily contradict the experimental observations because they do not take into account solvent effects that may preferentially stabilize the closed-shell singlet state. Moreover, it may not be necessary for the closed-shell state to be lower in energy than the open-shell, only that it is low enough so that the ISC matrix element is sufficiently large.

In this work, we have studied chloro-substituted phenylnitrenes (**1o**$^-$, **1m**$^-$, **1p**$^-$) by using negative ion photoelectron spectroscopy (NIPES). The studies were carried out using a newly constructed time-of-flight negative ion photoelectron spectrometer, which is described in detail.

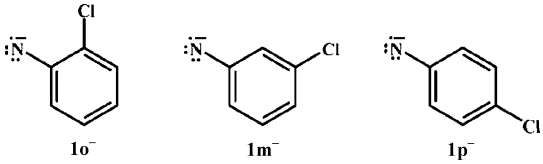

The measured photoelectron spectra agree with the computational studies[22] that chlorine substitution does not have a large effect on singlet−triplet energy splitting in aromatic nitrenes. However, the energies and band shapes of the singlet states indicate that chlorine substitution in the ortho- and para-positions surprisingly have non-negligible effects on the energies and geometries of the open-shell singlet states, presumably by resonance interactions.

Experimental Section

Photoelectron spectra of the phenylnitrene radical anions were measured by using a newly constructed time-of-flight negative ion photoelectron spectrometer at Purdue University (Figure 2). The experiment consist of four key processes: (1) ion formation, (2) mass analysis, (3) ion photodetachment, and (4) electron energy analysis. Details for each step are provided below.

(1) Ion Formation. Ions are formed in a pulsed expansion ionization source, similar to those described by Lineberger,[35−38] Johnson,[37,39−44] and Neumark.[45−47] Neutral precursors are introduced into the source chamber through a pulsed valve (General Valve, series 12). The head vapors from neutral samples are sealed in approximately 1 atm of Ar, which is used as a carrier gas. Less volatile samples are heated to increase the vapor pressure. Ionization is carried out by crossing the neutral pulse with a focused 600−700 V electron beam, generated in a home-built electron gun. Electron currents measured in a Faraday cup approximately 2 cm from the electron gun are ca. 300 μA. Ionization likely occurs by dissociative electron attachment by low-energy secondary electrons.[39,44,47]

The typical operating pressure in the ion source chamber is 4×10^{-5} Torr and the neutral precursors are cooled in the pulse expansion.[42] The absence of clear hot bands in the measured photoelectron spectra suggests the ions have low vibrational temperatures.

(2) Mass Analysis. Mass analysis is achieved by using a modified Wiley−McLaren type[48] time-of-flight mass spectrometer. The ions formed in the expansion are allowed to drift approximately 20 cm into the center of an extraction region, with an inner diameter of 19 cm. Ions are extracted by a −2200 V extraction pulse on the back plate in the extraction region, exiting through an orifice in the front plate. They then pass through a region of constant field that improves the resolution.[48] A second pulse of −1500 V is applied on either side of the constant-field region simultaneously with the extraction pulse. The ions then pass into the acceleration region. Shield rings are used to screen the ions from the walls of the vacuum chamber because the ratio of the plate spacing to their diameter is large. The rings in the extraction and acceleration regions are coupled to the front and back plates with a resistive/capacitive voltage divider network to maintain a linear electric field across the enclosed volume, while the plates and ring of the constant-field region are shorted together. The ions exit the acceleration region at ground potential, with average kinetic

energy of 1850 V. Timing is controlled by Model 555 Digital Delay-pulse Generator from Berkeley Nucleonics Corp.

The ions pass through an Einzel lens and a set of horizontal and vertical deflectors, into a differentially pumped, sealed vacuum chamber that serves as a field free region. The operating pressure in the second chamber is ca. 2×10^{-6} Torr. The ions enter into a differentially pumped back chamber (operating pressure is less than 1×10^{-6} Torr) through a 1 cm orifice and are detected with a 18 mm Advanced Bipolar detector from Burle Electro Optics Inc. (Sturbridge, MA). Analog ion currents are detected on an Agilent Infiniium Model 54810 A oscilloscope, triggered by the extraction pulse. The oscilloscope sends the information to the computer via a GPIB link. The computer is a PC running a LabVIEW application written in-house that controls the experiment and converts TOF data to mass spectra and/or electron kinetic energy.

(3) Photodetachment. Ions are photodetached approximately 15 cm before the ion detector by using the third harmonic output (355 nm = 3.493 eV) of a Lab170 Q-switched Nd:YAG laser (Spectra Physics: Mountain View, California). As the ions encounter the laser, electrons are ejected and the energies of these photodetached electrons will be used to generate the photoelectron spectrum (eq 2)

$$A^- + h\nu \rightarrow A + e^-(eKE) \qquad (2)$$

where A^- represents the anion that is intersected by the laser beam with excitation energy of $h\nu$, and the process will result formation of the neutral A and detached electron with kinetic energy, eKE.

For photodetachment to occur, the laser timing must be synchronized with the arrival of the mass selected anion. A screen set at −3 keV in front of the ion detector is used to allow only the neutrals formed during the detachment to reach the detector, allowing relatively easy tuning of the experimental parameters.

(4) Electron Energy Analysis. A small solid angle of photodetached electrons are detected at the end of a 1 m magnetically shielded flight tube. Electrons are detected using a second 18 mm Advanced Bipolar detector from Burle Electro Optics Inc. Photoelectron spectra are generated by plotting the number of measured electrons vs their time-of-flight. The relationship between kinetic energy, eKE, and the electron time-of-flight, t, is given by eq 3, where C and t_0 are calibrated by using a well-known system. A calibration spectrum (vide infra) is measured each day. Small energy differences due to differences in ion masses are not taken into account but are much smaller than the assigned uncertainties (0.05 eV).

$$eKE = \left(\frac{C}{t - t_0}\right)^2 \qquad (3)$$

(5) Electron Time-of-Flight to Energy Conversion. In this work, the time-of-flight to energy conversion is calibrated by using the photoelectron spectrum of phenylnitrene radical anion, **PhN**$^-$. The photoelectron spectrum of phenylnitrene radical anion was chosen for the calibration because the ion and resulting neutrals are structurally very similar to the chloro-substituted versions such that the photoelectron detachment behaviors should be expected to be similar. The photoelectron spectrum of **PhN**$^-$, previously reported by Ellison and co-workers,[24] contains bands for two electronic states, separated in energy by ca. 0.64 eV, with an adiabatic electron binding

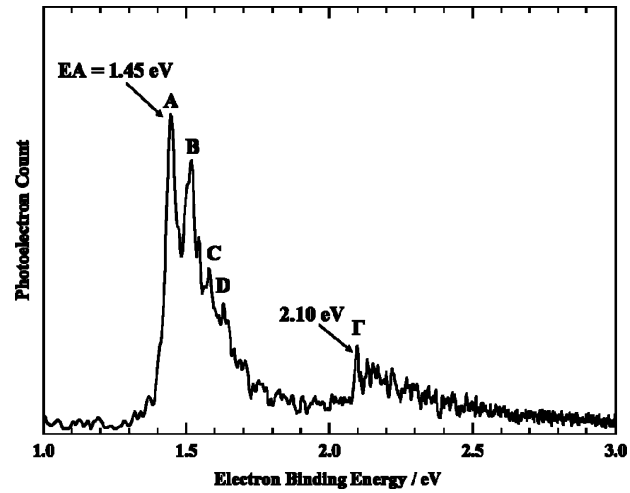

Figure 3. 355 nm photoelectron spectrum of phenylnitrene anion at 355 nm. Peak positions A, B, C, D, and Γ are set to be equal to those reported by Ellison and co-workers.[24]

energy of 1.45 eV for the lower energy state. The lower energy state also has a vibrational progression of approximately 500 cm^{-1}, which can be used to assess the resolution in the photoelectron spectra. Another advantage of using phenylnitrene for calibration is that nitrene anions are readily prepared by dissociative electron attachment (DEA) of the corresponding azides (eq 4).[15,18,24,25,49−51]

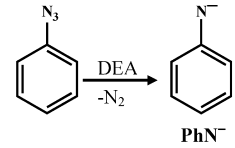

(4)

Unfortunately, the previously reported 488 nm photoelectron spectrum of **PhN**$^-$ did not have enough energy range to reveal the entire band for the singlet state. In their original paper, Travers et al.[24] report that the band is observed in an unpublished 351 nm photoelectron spectrum and assigned the weak peaks observed for the excited state in the 488 nm spectrum to hot bands for a more intense, singlet feature. However, the 355 nm photoelectron spectrum of **PhN**$^-$, measured using the Purdue NIPES instrument (Figure 3), does not show an intense excited state feature. A reanalysis of the 351 nm photoelectron spectrum cited by Ellison and co- workers[52] indicates that the intense feature described in the original work likely results from phenoxide impurity. The electron binding energy of the origin and the relative positions and intensities of the vibrational peaks agree with those reported by Gunion et al.,[53] and the mass of phenoxide ion, m/z 93, is similar to that of **PhN**$^-$ (m/z 91). Lastly, formation of phenoxide by reaction of PhN_3 with O^- is exothermic by 26 kcal/mol, so the ion can in principle be formed under flowing afterglow source conditions of the 351 nm NIPES experiment.

After accounting for the phenoxide impurity, there are still peaks in the 351 nm spectrum, which correspond to those originally assigned as hot bands in the 488 nm spectrum. These are likely not hot bands, but they are in fact part of the excited state spectral feature. An important implication of the reanalysis is that the singlet−triplet splitting phenylnitrene is revised to 0.64 ± 0.02 eV (14.8 ± 0.5 kcal/mol),[24] which is the energy difference between the origins of the triplet and singlet features in the 488 nm spectrum. The revised singlet−triplet splitting is

TABLE 1: Energies of the Peaks Observed in the 488 nm Photoelectron Spectrum of Phenylnitrene Anion[a]

electronic state	peak	electron binding energy, eV	vibrational energy,[b] cm^{-1}
triplet	A	1.45 ± 0.02	0
	B		500
	C		967
	D		1426
singlet	Γ	2.09 ± 0.02	0
	Δ		475

[a] Taken from ref 24. Labels correspond to peaks in the original report. [b] Peak position relative to the band origin.

in good agreement with the value of 15.9 kcal/mol predicted from high-level, multireference CI calculations.[17] The energies of all the peaks observed in photoelectron spectrum of **PhN**$^-$ are listed in Table 1. These peaks are observed in the Purdue spectrum of **PhN**$^-$ (Figure 3) and are used to create the energy scale calibration.

Materials

Unsubstituted and substituted phenyl azides were synthesized by literature procedures.[54] All the chemicals and reagents were obtained from commercial suppliers and were used as received.

Computational Methods

Electronic structure calculations of the anions and triplet states of the aromatic nitrenes were carried out using Gaussian 98W[55] and Gaussian 03W.[56] Geometries and frequencies were calculated at the B3LYP/aug-cc-pVTZ levels of theory. Electron affinities were calculated using the 0 K energies, which include zero point energy corrections. Zero point energies for each state were computed using the unscaled vibrational frequencies.

Results

Photoelectron Spectroscopy of I$^-$. To establish the capability of the new instrument to measure accurate electron affinities, we measured the photoelectron spectrum of I$^-$. Iodine has an accurately known electron affinity of 3.059 eV[57] and therefore is capable of being detached at 355 nm. The photoelectron spectrum, provided in the Supporting Information, shows a single peak with an electron kinetic energy of 0.440 eV, where the energy scale was calibrated by using the spectrum of phenylnitrene anion, as described above. The measured eKE indicates an electron affinity of 3.053 eV, in excellent agreement with the actual value.[57]

Photoelectron Spectra of (Chlorophenyl)nitrene Anions. The 355 nm photoelectron spectra of the (*o*-, *m*-, and *p*-chlorophenyl)nitrene anions are shown in Figure 4. The spectra are similar to each other and are similar to that measured for **PhN**$^-$ (Figure 3). Each spectrum shows two electronic states. By comparison with phenylnitrene, the more intense, lower energy feature is assigned to the triplet state, and the higher energy feature is assigned to the singlet. The peaks in the triplet state are close to Gaussian shaped, with a full-width-at-half-maximum of about 50 meV.

The assigned origin peaks of the triplet states are labeled A in each spectrum. Although some unresolved signal is observed at lower energies, particularly for the para-isomer, **1p**$^-$, it likely results either from hot bands or from dissociative detachment.[58−60] Photoelectron bands for the chlorophenylnitrene triplet states, predicted from calculated geometries of the ions and neutrals,[61] all indicate the origin peak to be the most intense peak in the spectrum, similar to what is observed for the unsubstituted phenylnitrene. The measured electron affinities of the chlorinated phenylnitrenes are listed in Table 2, along with the relative positions of the vibrational peaks observed in the triplet states. A slightly larger uncertainty is assigned for the para-isomer to account for the difficulty in assigning the origin peak.

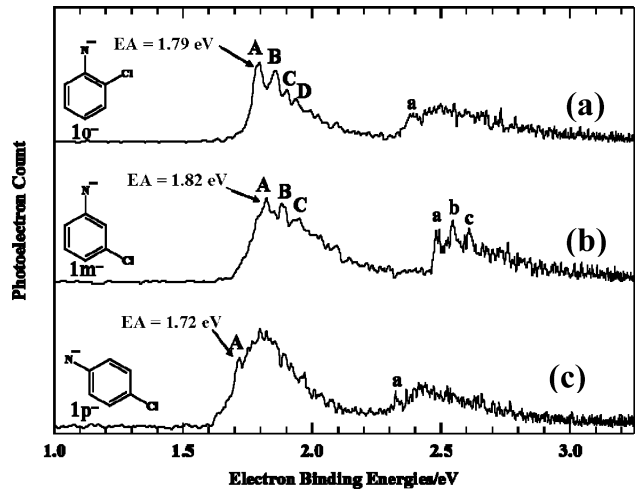

Figure 4. Photoelectron spectra of the (a) ortho-, (b) meta-, and (c) para-isomers of (chlorophenyl)nitrene anions at 355 nm. The region from 2.2 to 2.8 eV was scaled up by 2.5 to observe the origin of the singlet state more clearly. The origins of the triplet states are assigned as "A" and the other vibrational peaks are labeled as B−D. The origins of the singlet states are assigned as "a" for each isomer, and vibrational peaks are labeled b−c.

TABLE 2: Peaks Observed in the Photoelectron Spectra of 1o$^-$, 1m$^-$, and 1p$^-$ (Figure 4)

isomer	electronic state	peak	electron binding energy, eV	vibrational energy,[a] cm^{-1}
1o	triplet	A	1.79 ± 0.05	0
		B		500
		C		900
		D		1200
	singlet	a	2.38 ± 0.10	0
1m	triplet	A	1.82 ± 0.05	0
		B		500
		C		950
	singlet	a	2.47 ± 0.05	0
		b		600
		c		900
1p	triplet	A	1.72 ± 0.10	0
	singlet	a	2.31 ± 0.10	0

[a] Estimated uncertainties are ± 100 cm^{-1}.

The origin of the singlet is easily identified for the meta-substituted ion and labled "a" in Figure 4b. The singlet states of the ortho- and para-isomers, however, are not well-resolved. In these systems, the origins of the singlet states are estimated as the energies where the signals begin to be observed, technically corresponding to upper limits to the origin energies. Larger uncertainties (0.1 eV) are assigned to the origin assignments for singlet states of **1o** and **1p**. The singlet state origins and observed vibrational peaks are listed in Table 2.

Computational Studies. Electronic structure calculations were carried out to investigate the electronic states of **1o**$^-$, **1m**$^-$, and **1p**$^-$ and the electron affinities of the triplet nitrenes. Optimized geometries and the full list of calculated frequencies are included as Supporting Material. The electronic structures of the phenylnitrene radical anions can be viewed as resulting from adding an electron to the corresponding phenylnitrenes.

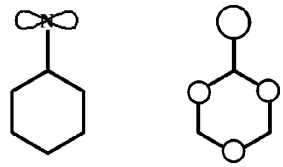

Figure 5. σ and π orbitals in phenylnitrene.

TABLE 3: Measured and Calculated Thermochemical Properties for Chlorophenylnitrenes

electron affinity, eV (measured)	electron affinity, eV (calculated)[a]	ΔE_{ST}, kcal/mol (measured)	ΔE_{ST}, kcal/mol (calculated)[b]	
1o	1.79 ± 0.05	1.79	14 ± 2	
1m	1.82 ± 0.05	1.84	15 ± 1	14.3
1p	1.72 ± 0.05	1.71	14 ± 2	13.7

[a] Values calculated at the B3LYP/aug-cc-pVTZ level of theory, using the isodesmic approach shown in eq 5. [b] Reference 22.

There are two electronic states that can be formed for the ion, by adding an electron to either the singly occupied σ or π orbitals in the triplet, shown in Figure 5. In C_s symmetry, this results in either a $^2A'$ ($\pi^2\sigma$) or $^2A''$ ($\sigma^2\pi$) electronic state.[22,24] In phenylnitrene and **1p**, which have C_{2v} symmetry, the $\pi^2\sigma$ and $\sigma^2\pi$ states are $^2B_1$ and $^2B_2$, respectively.[15] Energies were calculated at the B3LYP/aug-cc-pVDZ levels of theory. For all of the phenylnitrene radical anions, the A′ ($\pi^2\sigma$) state is calculated to be lower in energy than the A″ ($\sigma^2\pi$) state, by ca. 0.7 eV. Adiabatic electron affinities of the chlorinated phenylnitrenes were obtained by adding the calculated 0 K energy for the reaction shown in eq 5, using the ground state energies of the ions and neutrals, to the experimental EA of phenylnitrene, 1.45 ± 0.02 eV,[24] and are listed in Table 3.

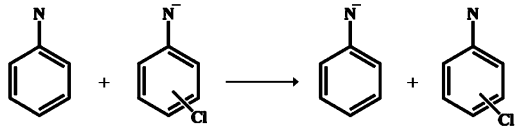

(5)

Discussion

Triplet States and Electron Affinities. The measured electron affinities of the triplet phenylnitrenes are in excellent agreement with the values predicted by electronic structure calculations (Table 3). The largest EA is found for the meta-isomer, **1m**, with **1p** having the smallest. The trend in the EAs is the same as that observed previously by Kim et al., for benzyl radicals,[62] and is consistent with what is expected given the electronic effects of the chlorine substituent. As a π donor, it destabilizes the negative ion when it is in resonant positions (ortho and para), which lowers the EA compared to that for the meta-isomer. However, it also stabilizes the ion, albeit to a lesser extent, by an inductive effect, and the ortho-anion is stabilized more than the para because the chlorine is closer to the charge center.

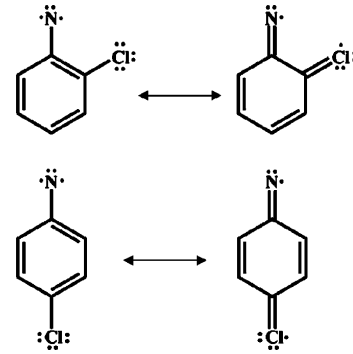

Figure 7. Quinoidal resonance structures for the open-shell states of **1p**. Similar structures can be drawn for the ortho-isomer, **1o**.

Vibrational peaks are observed in the triplet bands for the ortho- and meta-isomers. The vibrational progressions are ca. 400−500 cm^{-1} for both states. The vibrational mode active in these spectra is likely a ring deformation mode. Similar vibrational progressions have been observed in photoelectron spectra of other aromatic systems.[62−64] Possible vibrational modes, calculated at the B3LYP/aug-cc-pVTZ level of theory, are shown in Figure 6.

Singlet States. Dramatic differences are observed in the singlet state features for the meta-isomer compared to the ortho- and para-isomers. The band for the meta-isomer is well-resolved, with a well-defined origin and observable vibrational structure. The vibrational spacing is ca. 500 cm^{-1}, similar to that found in the triplet state. In contrast, the singlet states for the ortho- and para-isomers do not have resolved peaks.

The difference in the singlet features for the isomers suggest differences in the Franck−Condon factors for the photodetachment. The isomeric dependence suggests that the geometry differences result from a resonance interaction between the ring/nitrene and the substituent. For example, as described in the Introduction quinoidal resonance structures are possible for the ionic states of **1o** and **1p**, which would lead to very large geometry difference for the singlet state. However, calculations by Cramer and co-workers[22] predict the open-shell singlet to be the lowest energy singlet states for all three nitrenes, similar to phenylnitrene itself, with the ionic states much higher in energy. As such, the ionic states do not likely account for the obtained features.

As shown in Figure 7, quinoidal structures are also possible for the open-shell singlet states of the ortho- and para-chlorinated phenylnitrenes. The advantage of this type of electronic structure for the open-shell singlet states is that the unpaired electrons

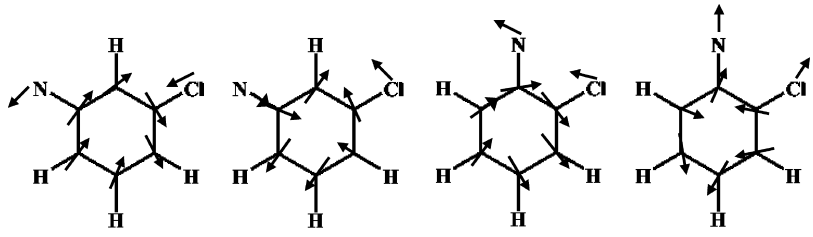

Figure 6. Triplet state ring deformation vibrational modes potentially active in the photoelectron spectra of (chlorophenyl)nitrene anions. Vibrational frequencies calculated at the B3LYP/aug-cc-pVTZ level of theory.

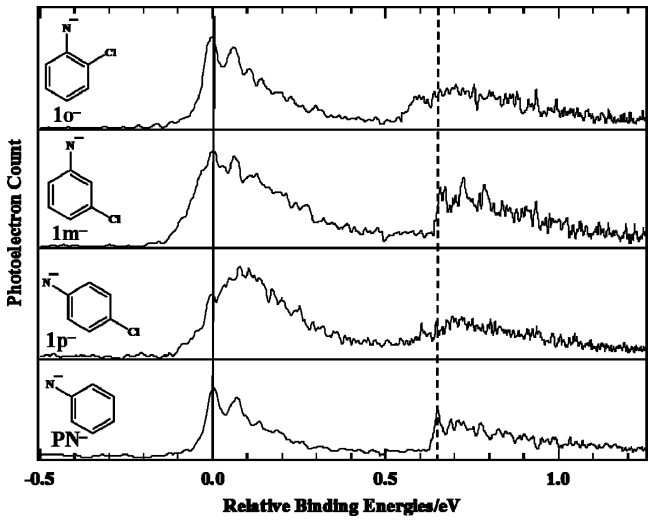

Figure 8. Relative photoelectron spectra of phenylnitrene and (chlorophenyl)nitrene anions. The regions from 0.5 to 1.1 were scaled up by 2.5. The solid line at 0.0 eV indicates the origins of the triplet states, and the dashed line indicates singlet state origin of the unsubstituted phenylnitrene.

are localized on separate atoms in the molecules. Borden and Davidson[65] have described how singlet states of diradicals are destabilized by electron repulsion when the orbitals have atoms in common, and the repulsion can be minimized by spatially separating the electrons as in the quinoidal structures. In contrast, local exchange interaction in the triplet favors the structures where the unpaired electrons are localized on the same atom, so the quinoidal structures would not be beneficial for the triplet state. Consequently, geometry differences are expected between the singlet and triplet states of the ortho- and para-subsituted nitrenes. Because the meta-position is not in resonance with the nitrenes, substitution at that position should not affect the structure of the open-shell singlet state.

The contribution of the quinoidal structures appears to provide energy stabilization to the open-shell singlet states. The measured singlet−triplet splitting in **1o** and **1p** (Table 3) are slightly smaller than those in **1m** and **PhN**. The relative singlet−triplet energy gaps for the **1m** and **1p** agree with the calculated values reported at the DFT level of theory by Cramer and co-workers.[22] The differences in the singlet−triplet splitting are more clearly apparent in Figure 8, where the spectra are plotted relative to the origins of the triplet states. In this representation, it can be seen that the vertical detachment energies for the singlet states are similar, whereas the relative band origins for the **1o** and **1p** are at lower energies.

The substituent effect can also be understood from a molecular orbital perspective. The π molecular orbitals for the chlorinated nitrene are formed by the combination of the nitrene- and chlorine-based benzylic orbitals, as shown in Figure 9. The symmetric and antisymmetric combinations of the two benzylic-like orbitals create the bonding and antibonding orbitals of the quinoidal structure. For the open-shell singlet, the antibonding orbital is singly occupied (Figure 9). In the MO description, the reduction in the electron-pair repulsion in the singlet is accomplished by delocalization of the spin in the π orbital (the other unpaired electron is localized in a nitrogen σ orbital). The MO description also explains the apparent "octet rule" violation in the quinoidal resonance structure and shows that it does not require an "expanded octet" model, such that it is not specific to chlorine or second row substituents.

The effect of spin-repulsion on the structure of the open-shell singlet state of **PhN** has been discussed previously by

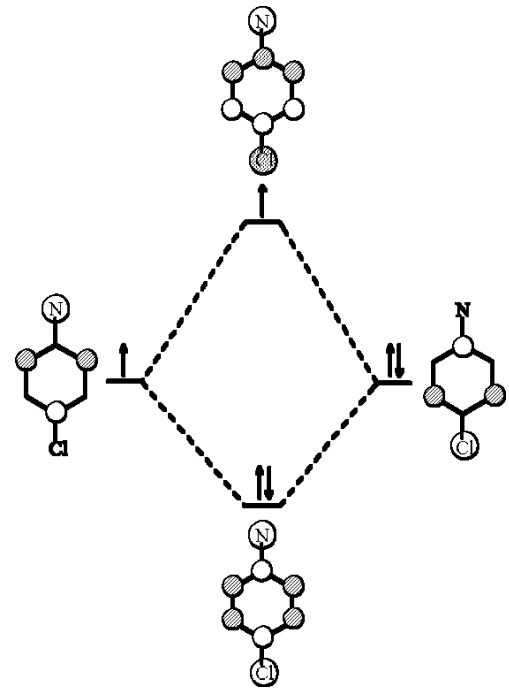

Figure 9. Schematic MO diagram showing the effect of chlorine substitution. The MO pictures are qualitative symmetry-adapted versions and do not necessarily represent the orbital coefficients in the LCAO.

Karney and Borden,[23] who argued that the open-shell singlet is best represented by the structure shown in **2**, where the π-radical is localized in the aromatic ring. Adding the chlorine substituent to the ortho- or para-positions of **2** results in additional geometry deformation, as in the quinoidal structures shown in Figure 8.

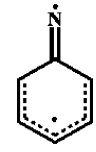

2

Conclusions

The experimental electron affinities for the ortho-, meta-, and para-subsituted (chlorophenyl)nitrenes are 1.79 ± 0.05, 1.82 ± 0.05, and 1.72 ± 0.05 eV, respectively, and are in good agreement with theoretical predictions. Introduction of a chlorine substituent onto the phenylnitrene ring does not change the electronic structure of lowest energy singlet states, which are open-shell states. The singlet−triplet energy gaps are not significantly affected by the chlorine substitution, but subtle changes are observed in bands for the ortho- and para-singlet states, likely due to the resonance interactions in the open-shell singlet.

Acknowledgment. This work was supported by the National Science Foundation (CHE04-54874 and CHE08-08964). We thank the donors of the Petroleum Research Fund, administered by the American Chemical Society, for partial support. We also thank Profs. Barney Ellison and Carl Lineberger (University of Colorado) for providing access to the 351 nm spectrum of phenylnitrene anion and for useful conversations, Prof. Anna Krylov (USC) for assistance with predicting the photoelectron

spectra, and Mr. Daniel Cruz-Ramirez for assistance collecting the I^- spectrum.

Supporting Information Available: Photoelectron spectrum of I^-. **Z**-matrices and calculated energies,and full refs 13, 40, 55, and 56. This material is available free of charge via the Internet at http://pubs.acs.org.

References and Notes

(1) Borden, W. T.; Gritsan, N. P.; Hadad, C. M.; Karney, W. L.; Kemnitz, C. R.; Platz, M. S. *Acc. Chem. Res.* **2000**, *33*, 765–771.
(2) Gritsan, N. P.; Platz, M. S. *Adv. Phys. Org. Chem.* **2001**, *36*, 255–304.
(3) Karney, W. L.; Borden, W. T. *Adv. Carbene Chem.* **2001**, *3*, 205–251.
(4) Platz, M. S. *Acc. Chem. Res.* **1995**, *28*, 487–492.
(5) Platz, M. S.; Leyva, E.; Haider, K. *Org. Photochem.* **1991**, *11*, 367–429.
(6) Gutsche, C. D.; Bachman, G. L.; Coffey, R. S. *Tetrahedron* **1962**, *18*, 617–627.
(7) Closs, G. L.; Moss, R. A. *J. Am. Chem. Soc.* **1964**, *86*, 4042–4053.
(8) Kirmse, W.; Hoemberger, G. *J. Am. Chem. Soc.* **1991**, *113*, 3925–3934.
(9) Meijer, E. W.; Nijhuis, S.; van Vroonhoven, F. C. B. M. *J. Am. Chem. Soc.* **1988**, *110*, 7209–7210.
(10) Bauschlicher, C. W. *Chem. Phys. Lett.* **1980**, *74*, 273–276.
(11) Dannenberg, J. J.; Vinson, L. K.; Moreno, M. B. J. *J. Org. Chem.* **1989**, *54*, 5487–5491.
(12) Moss, R. A.; Dolling, U. H. *J. Am. Chem. Soc.* **1971**, *93*, 954–960.
(13) Nimlos, M. R.; et al. *J. Chem. Phys.* **2002**, *117*, 4323–4339.
(14) Wasserman, E. *Prog. Phys. Org. Chem.* **1971**, *8*, 319–336.
(15) Drzaic, P. S.; Brauman, J. I. *J. Am. Chem. Soc.* **1984**, *106*, 3443–3446.
(16) Wasserman, E.; Smolinsky, G.; Yager, W. A. *J. Am. Chem. Soc.* **1964**, *86*, 3166–3167.
(17) Winkler, M. *J. Phys. Chem. A* **2008**, *112*, 8649–8653.
(18) McDonald, R. N.; Davidson, S. J. *J. Am. Chem. Soc.* **1993**, *115*, 10857–10862.
(19) Reiser, A.; Leshon, L. J. *J. Am. Chem. Soc.* **1971**, *93*, 4051–4052.
(20) Smolinsky, G.; Wasserman, E.; Yager, W. A. *J. Am. Chem. Soc.* **1962**, *84*, 3220–3221.
(21) Hrovat, D. A.; Waali, E. E.; Borden, W. T. *J. Am. Chem. Soc.* **1992**, *114*, 8698–8699.
(22) Johnson, W. T. G.; Sullivan, M. S.; Cramer, C. J. *Int. J. Quantum Chem.* **2001**, *85*, 492–508.
(23) Karney, W. L.; Borden, W. T. *J. Am. Chem. Soc.* **1997**, *119*, 1378–1387.
(24) Travers, M. J.; Cowels, D. C.; Clifford, E. P.; Ellison, G. B. *J. Am. Chem. Soc.* **1992**, *114*, 8699–8701.
(25) Travers, M. J.; Cowles, D. C.; Clifford, E. P.; Ellison, G. B.; Engelking, P. C. *J. Chem. Phys.* **1999**, *111*, 5349–5360.
(26) Kemnitz, C. R.; Karney, W. L.; Borden, W. T. *J. Am. Chem. Soc.* **1998**, *120*, 3499–3503.
(27) Cramer, C. J.; Dulles, F. J.; Falvey, D. E. *J. Am. Chem. Soc.* **1994**, *116*, 9787–9788.
(28) Matzinger, S.; Bally, T.; Patterson, E. V.; McMahon, R. J. *J. Am. Chem. Soc.* **1996**, *118*, 1535–1542.
(29) Schreiner, P. R.; Karney, W. L.; Schleyer, P. V. R.; Borden, W. T.; Hamilton, T. P.; Schaefer, H. F., III. *J. Org. Chem.* **1996**, *61*, 7030–7039.
(30) Wong, M. W.; Wentrup, C. *J. Org. Chem.* **1996**, *61*, 7022–7029.
(31) Gritsan, N. P.; Zhendong, Z.; Hadad, C. M.; Platz, M. S. *J. Am. Chem. Soc.* **1999**, *121*, 1202–1207.
(32) Salem, L.; Rowland, C. *Angew. Chem., Int. Ed. Engl.* **1972**, *11*, 92.
(33) Albini, A.; Bettinetti, G.; Minoli, G. *J. Am. Chem. Soc.* **1999**, *121*, 3104–3113.
(34) Gritsan, N. P.; Tigelaar, D.; Platz, M. S. *J. Phys. Chem. A* **1999**, *103*, 4465–4469.
(35) Alexander, M. L.; Johnson, M. A.; Lineberger, W. C. *J. Chem. Phys.* **1985**, *82*, 5288–5290.
(36) Alexander, M. L.; Johnson, M. A.; Levinger, N. E.; Lineberger, W. C. *Phys. Rev. Lett.* **1986**, *57*, 976–979.
(37) Johnson, M. A.; Lineberger, W. C. *Techniques for the Study of Gas-phase Ion Molecule Reactions*; Farrar, J. M., Saunders, W. H. , Eds.; Wiley: New York, 1988; p 591.
(38) Johnson, M. A.; Alexander, M. L.; Lineberger, W. C. *Chem. Phys. Lett.* **1984**, *112*, 285–290.
(39) Hammer, N. I.; Roscioli, J. R.; Johnson, M. A. *J. Phys. Chem. A* **2005**, *109*, 7896–7901.
(40) Ichihashi, M.; et al. *J. Phys. Chem.* **1995**, *99*, 1655–1659.
(41) Kim, J.; Kelley, J. A.; Ayotte, P.; Nielsen, S. B.; Weddle, G. H.; Johnson, M. A. *J. Am. Soc. Mass Spectrom.* **1999**, *10*, 810–814.
(42) Posey, L. A.; Deluca, M. J.; Johnson, M. A. *Chem. Phys. Lett.* **1986**, *131*, 170–174.
(43) Weber, J. M.; Kim, J.; Woronowicz, E. A.; Weddle, G. H.; Becker, I.; Cheshnovsky, O.; Johnson, M. A. *Chem. Phys. Lett.* **2001**, *339*, 337–342.
(44) Weber, J. M.; Robertson, W. H.; Johnson, M. A. *J. Chem. Phys.* **2001**, *115*, 10718–10723.
(45) Kitsopoulos, T. N.; Waller, I. M.; Loeser, J. G.; Neumark, D. M. *Chem. Phys. Lett.* **1989**, *159*, 300–306.
(46) Metz, R. B.; Kitsopoulos, T.; Weaver, A.; Neumark, D. M. *J. Chem. Phys.* **1988**, *88*, 1463–1465.
(47) Metz, R. B.; Weaver, A.; Bradforth, S. E.; Kitsopoulos, T. N.; Neumark, D. M. *J. Phys. Chem.* **1990**, *94*, 1377–1388.
(48) DeHeer, W. A.; Milani, P. *Rev. Sci. Instrum.* **1991**, *62*, 670–677.
(49) Drzaic, P. S.; Brauman, J. I. *J. Phys. Chem.* **1984**, *88*, 5285–5290.
(50) McDonald, R. N.; Chowdhury, A. K.; Setser, D. W. *J. Am. Chem. Soc.* **1981**, *103*, 6599–6603.
(51) McDonald, R. N.; Chowdhury, A. K. *J. Am. Chem. Soc.* **1980**, *102*, 5118–5119.
(52) Ellison, G. B.; Lineberger, W. C., private communication.
(53) Gunion, R. F.; Gilles, M. K.; Polak, M. L.; Lineberger, W. C. *Int. J. Mass Spectrom.* **1992**, *117*, 601–620.
(54) Faucher, N.; Ambroise, Y.; Cintrat, J. C.; Doris, E.; Pillon, F.; Rousseau, B. *J. Org. Chem.* **2002**, *67*, 932–934.
(55) Frisch, M. J. *Gaussian 98*, revision A.09; Gaussian, Inc.: Pittsburgh, PA, 1998.
(56) Frisch, M. J., *Gaussian 03*, revision D.01; Gaussian, Inc.: Wallingford, CT, 2004.
(57) Hanstrop, D.; Gustafsson, M. *J. Phys. B: At. Mol. Opt. Phys.* **1992**, *25*, 1773–1783.
(58) Bowen, M. S.; Becucci, M.; Continetti, R. E. *J. Phys. Chem. A* **2005**, *109*, 11781–11792.
(59) Bowen, M. S.; Becucci, M.; Continetti, R. E. *J. Chem. Phys.* **2006**, *125*, 133309/133301–133309/133309.
(60) Lu, Z.; Hu, Q.; Oakman, J. E.; Continetti, R. E. *J. Chem. Phys.* **2007**, *126*, 194305/194301–194305/194311.
(61) Krylov, A. I., Koziol, L. Private Communication.
(62) Kim, J. B.; Wenthold, P. G.; Lineberger, W. C. *J. Phys. Chem. A* **1999**, *103*, 10833–10841.
(63) Wenthold, P. G.; Squires, R. R.; Lineberger, W. C. *J. Am. Chem. Soc.* **1998**, *120*, 5279–5290.
(64) Leopold, D. G.; Miller, A. E. S.; Lineberger, W. C. *J. Am. Chem. Soc.* **1986**, *108*, 1379–1384.
(65) Borden, W. T.; Davidson, E. R. *J. Am. Chem. Soc.* **1977**, *99*, 4587–4594.

JP9039594